Computational Modeling of the Interaction of Molecular Oxygen with the Flavin-dependent Enzyme RutA

Igor V. Polyakov[1,2] iD *, Tatiana M. Domratcheva*[1] iD *, Anna M. Kulakova*[1] iD *, Alexander V. Nemukhin*[1,2] iD *, Bella L. Grigorenko*[1,2] iD

Supercomputer molecular modeling methods are applied to characterize structure and dynamics of the flavin-dependent enzyme RutA in the complex with molecular oxygen. Following construction of a model protein system, molecular dynamics (MD) simulations were carried out using either classical force field interaction potentials or the quantum mechanics/molecular mechanics (QM/MM) potentials. Several oxygen-binding pockets in the protein cavities were located in these simulations. The QM/MM-based MD calculations rely on the interface between the quantum chemistry package TeraChem and the MD package NAMD. The results show a stable localization of the oxygen molecule in the enzyme active site. Static QM/MM calculations carried out with two different packages, NWChem and TURBOMOLE, allowed us to establish the structure of the RutA-O_2 complex. Biochemical perspectives of the hallmark reaction of incorporating oxygen into organic compounds emerged from these simulations are formulated.

Keywords: computational modeling, molecular dynamics, quantum mechanics/molecular mechanics, protein-oxygen interaction, flavin-dependent enzymes.

Introduction

Modeling vitally important reactions of biomolecules with molecular oxygen is one of the most demanding subjects in life sciences. In particular, it is necessary to account for activation of the initially chemically inert molecule O_2 in the triplet spin state in order to obtain chemically reactive species. Computer simulations of elementary steps of the oxidation reactions require application of various modeling tools, including construction of all-atom three-dimensional model systems, preliminary relaxation of geometry parameters with the help of large-scale classical molecular dynamics (MD) simulations, and application of the quantum-based methods to locate stationary points on the potential energy surfaces of different spin multiplicity to estimate transition energies between electronic states, and to scan energy profiles along properly selected reaction coordinates. Application of the quantum mechanics/molecular mechanics (QM/MM) theory is an essential step in these simulations, which require high-performance supercomputer facilities [21].

An additional requirement in studies of the oxygen-binding proteins is to characterize the accommodation of O_2 in the protein cavities, because the localization of oxygen in these sites is a nontrivial experimental task. Only few structures in the Protein Data Bank [7] report complexes of proteins with molecular oxygen, e.g., [5, 10, 18]. It should be also pointed out that the resulting experimental electron density is produced using computational refinement [24] before deposition to the structure databanks. Thus, computer simulations are indispensable for revealing structures of the oxygen-binding proteins. In this work, we demonstrate the achievements and the problems of the required computational procedures when considering interaction of O_2 with the flavin-dependent enzyme RutA from *Escherichia coli* as an important example.

Flavin-binding monooxygenase RutA, catalyzing critical steps in degradation of uracil [16], has been characterized by preforming O_2 pressurized crystallography experiments and a specific

---

[1]Department of Chemistry, Lomonosov Moscow State University, Moscow, Russian Federation
[2]Emanuel Institute of Biochemical Physics, Russian Academy of Sciences, Moscow, Russian Federation

O_2 binding site has been suggested on the basis of these experiments [18]. RutA and other monooxygenases employ flavin cofactors derived from riboflavin (vitamin B2) in the form of flavin mononucleotide (FMN) or flavin-adenine dinucleotide that share the reactive isoalloxazine ring and adopt various redox states of the system [26]. In general, the interaction of O_2 with flavin cofactors in flavoproteins is of a particular importance for biochemistry [1, 17].

1. Molecular Model Setup

We explore the recently published crystal structure PDB ID 6SGG [18] as an initial guess of atomic coordinates of heavy atoms in the construction of the model system. According to the reported data, the protein structure contains the non-covalently bound FMN cofactor and the oxygen molecule near the isoalloxazine ring of FMN. In our simulations, hydrogen atoms were added assuming the conventional protonation states of the polar residues Arg, Lys (positively charged), Glu, Asp (negatively charged), at neutral pH. The histidine residues were assumed in the neutral state. The loop Glu292 - Ala310, which is poorly defined in the crystal structure, was manually refined. Topology files for the protein for MD simulations were constructed using the psfgen toolkit of NAMD [22]. The force field parameters correspond to the CHARMM36 library [8]. Parameters of the FMN molecule in the reduced form (with the total charge -3 e) were taken from Ref. [3] and those for the molecular oxygen were taken from Ref. [29]. Water molecules resolved in the crystal structure were kept in the model system, while solvation water shells were built using the visual molecular dynamics (VMD) plugins [13], the TIP3P water model was employed. The model system composed of 42174 atoms in total.

The constructed model system is illustrated in the main frame in Fig. 1 showing the secondary structure of the RutA protein (α-helices and β-sheets), the FMN molecule without hydrogen atoms, and the oxygen molecule. The inset in Fig. 1 shows the all-atom model of FMN and the O_2 molecule near the isoalloxazine ring. The atoms of the latter, N5 and C4a, are considered as competing sites for flavin oxidation, according to the current dispute [18].

Classical MD simulations were carried out using the NAMD 3.0 software package [22]. The isothermal-isobaric (NPT) ensemble at P = 1 atm and T = 300 K using the Nosé-Hoover Langevin piston pressure control and the Langevin dynamics were employed. Integration step was set to 1 fs. Periodic boundary conditions and the particle mesh Ewald algorithm to account for the long-range electrostatic interactions were applied, whereas the non-bonded interaction cut-off parameter was set to 12 Å. The solvation water box was equilibrated in a short 1 ns calculation while keeping the protein heavy atoms fixed. The use of NAMD allowed us to efficiently utilize the DGX-2 supercomputer. The node configuration included Dual Intel Xeon Platinum 8168, 1.5 TB RAM, 16 NVIDIA Tesla V100 GPUs (NVSwitch interconnect) and a 30 TB NVMe RAID0 SSD storage. We ran a swarm of 8 trajectories simultaneously on a single DGX-2 node, while only 8 CPU cores were utilized. This is possible with the new GPU-resident version of NAMD 3.0 with the CUDASOAintegrate option set to "on". Our benchmark showed that at maximum, 16 parallel trajectories can be executed to exploit all the V100 GPUs of a DGX-2 node, which results in a performance of over 1000 ns/day for model systems considered in this work.

Panels in Fig. 2 illustrate the main conclusions, which can be drawn from classical MD simulations. Panel (a) reports that the overall protein structure remains stable throughout the classical MD trajectories, the graph shows the root mean square deviation (RMSD) calculated
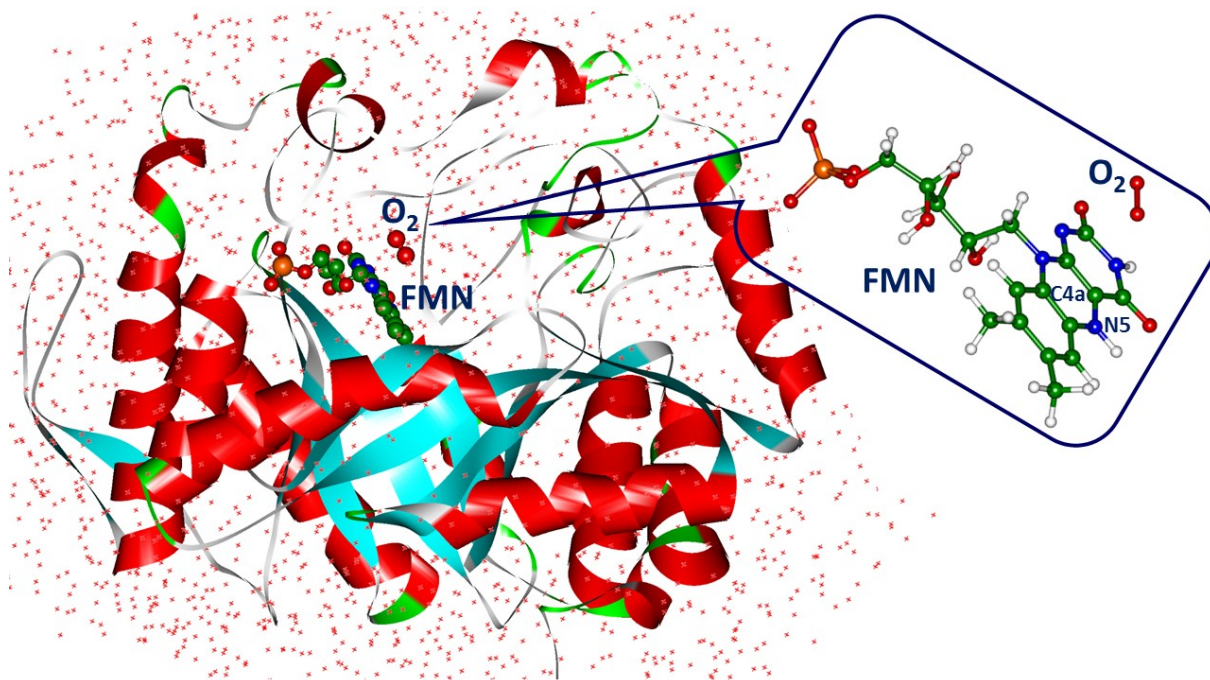
Figure 1. Computationally derived model system of the RutA protein with the FMN cofactor and the oxygen molecule. Conventionally, α-helices of the protein are shown in red, β-sheets in cyan. The red dots surrounding the protein refer to solvation water shells. The inset in the right part shows the FMN-O_2 species with the hydrogen atoms. Carbon atoms are colored green, oxygen – red, nitrogen – blue, phosphorus – orange, hydrogen – white. C4a and N5 atoms form a covalent bond

over the CA atoms of the amino acid residues in a typical run. Panel (b) reports that the non-covalently bound FMN cofactor remains in a single stable conformation as well.

The most important finding refers to the location of the O_2 molecule. The calculations show (see Fig. 2) that the molecule is localized in different protein pockets in MD runs. Pocket-1 roughly corresponds to the arrangement identified in the crystal structure PDB ID 6SGG. Here, the oxygen molecule fluctuates in the region between the flavin moiety, polar residues Asn134, Thr105 and a hydrophobic cluster of Leu65, Met67 and Phe25 sidechains. The retention time of oxygen in any pocket varies from hundreds of picoseconds to tens of nanoseconds. We notice that along the MD trajectories, the oxygen species tends to move from pocket-1 to pocket-2 or pocket-5. In pocket-5, the O_2 molecule is surrounded by water molecules and resides closer to the C4a atom of the flavin molecule (see Fig. 1). Pocket-2 is mostly hydrophobic; it is formed by the sidechains of Asn134, Phe224, Ala206, Leu65 and flavin. Pocket-3 consists of the sidechains Phe222, Phe224, Tyr257, Ile204, Phe63; it is close to the protein outer surface, showing one of the obvious ways connecting the pocket-1 (identified in the crystal structure) to the bulk, $1 \rightarrow 2 \rightarrow 3$. Pocket-4 is formed by the FMN phosphate group, the Tyr160, Cys205 sidechains and nearby main chain of β-strands. From the practical point of view, classical MD simulations with the CHARMM36 force field described here are feasible for conformational sampling in this complicated biomolecular system. However, these simulations lack to describe an important feature of this system, that is to model a partial electron transfer from the reduced FMN moiety to the O_2 species [5]. Therefore, we consider MD simulations for this complex with the QM/MM potentials, that is the QM/MM MD approach.
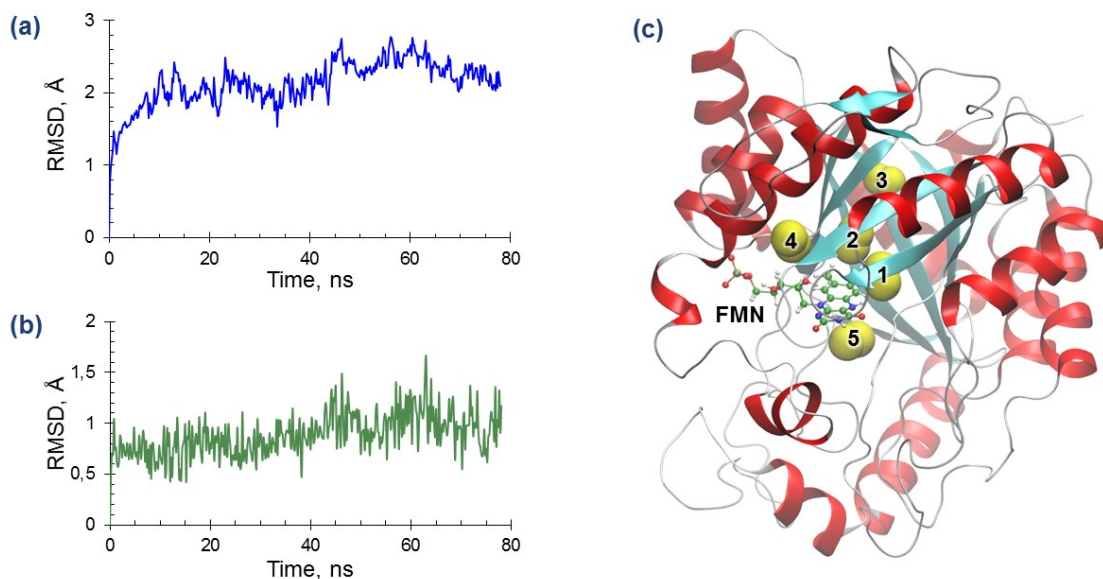
Figure 2. The results obtained in classical MD simulations: (a) RMSD over the CA atoms during a classical MD trajectory; (b) RMSD over the heavy atoms of FMN (in both cases, a, and b, the alignment was performed for the protein backbone in all the frames relative to the crystal structure PDB ID 6SGG); (c) the located pockets in protein cavities for the O_2 molecule shown by pairs of large yellow balls

2. QM/MM MD Simulations

The QM/MM MD trajectories were initiated from the frames of classical MD in the vicinity of pocket-1. We assigned to the quantum subsystem the oxygen molecule and the atoms from the molecular groups from the isoalloxazine ring of FMN, Asn134 and Thr105 side chains (see Fig. 3). The QM part consisted of 56 atoms in total, and it was treated at the density functional theory (DFT) level with the range-separated ωB97X functional [9] and the D3 dispersion correction [12]. The 6-31G** basis set was employed for carbon and hydrogen atoms and 6-31+G** for nitrogen and oxygen atoms. The QM subsystem was treated in the triplet state due to the ground electronic state of O_2 using the unrestricted DFT approach. The remaining atoms of the model system were assigned to the MM part described by the CHARMM36 [8] force field. Presently, MD simulations with the QM/MM potentials benefit greatly from the GPU systems because of the use of the software stack of TeraChem [23] and NAMD [22] with the appropriate interfaces. The originally implemented interface [19] had some pitfalls, which were recently fixed [14].

The present simulations were carried out on 8 GPUs in parallel resulting in a combined 172 ps trajectory. The measured performance was $\approx$2.5 ps per day on a single GPU or 40 ps per single DGX-2 node.

The important results of these simulations are as follows. First, we observe a significant electron density transfer to the O_2 molecule from FMN. For instance, the amount of the Mulliken charge on the O_2 moiety was up to 0.4 e, when O1-N5 or O2-N5 distances were less than 3 Å. Second, the graph of distances between the oxygen atoms in O_2 and the N5 atom in the isoalloxazine ring of FMN shown in the right part in Fig. 3 demonstrates that the oxygen molecule stably resides in the protein. Third, this graph predicts a N5-O1/O2 distance of 3.5 Å,
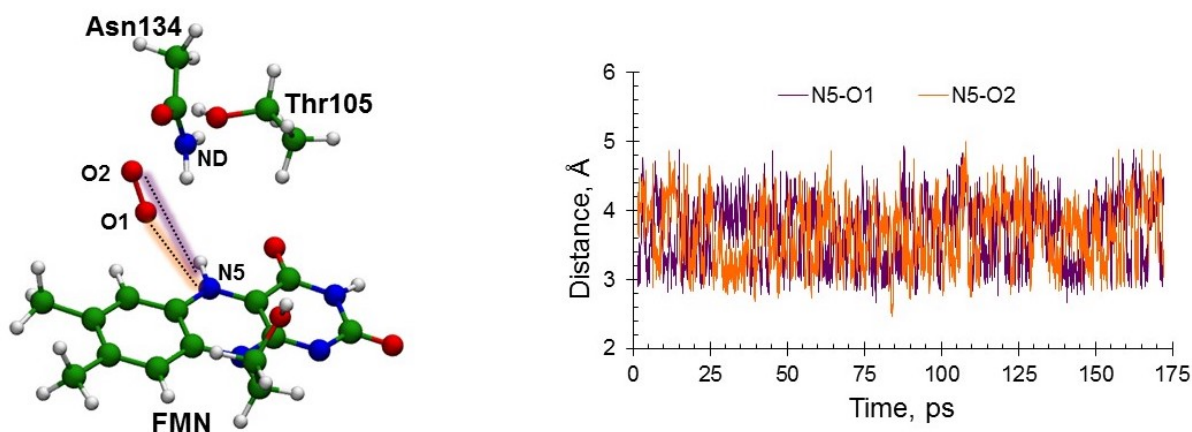
Figure 3. Left – quantum subsystem in the QM/MM MD calculations. Right – graph of the distances between the oxygen atoms in O_2 and the N5 atom in the isoalloxazine ring of FMN along the QM/MM MD trajectories

which is significantly longer that the distance 2.09 Å observed in the parent crystal structure PDB ID 6SGG [18]. Hence, we observe a clear discrepancy in the experimentally determined and computed O-N5 distances.

3. QM/MM Calculations

In this subsection, we report the results of static QM/MM calculations carried out to locate the minimum energy points on the potential energy surface of the RutA-O_2 complexes using two different quantum chemistry software packages. We note that QM/MM simulations are less demanding in computational efforts as compared to the QM/MM MD approach. For instance, a micro iterative structure optimization in QM/MM requires approximately 10^2 energy-gradient calculations, whereas a mere 10 ps QM/MM MD trajectory requires 10^4 such calculations. Nevertheless, QM/MM simulations, which rely on *ab initio*-type quantum chemistry approaches in QM, are still quite expensive for biomolecular systems composed of thousands atoms as in our case.

First, we describe the use of a modern computer based on a consumer-grade 16 core Ryzen 5950x CPU. We applied the software stack of Tcl ChemShell [25] with the efficient DL-FIND optimizer [15] and TURBOMOLE quantum chemistry software package [6]. ChemShell was compiled on Ubuntu Linux 18.04 using gfortran/gcc version 7.5, OpenMPI v. 2.1.1. Preliminary testing showed that this strategy is very efficient for QM/MM calculations.

In the TURBOMOLE/ChemShell calculations, the same QM-MM partitioning was assumed for the protein with the FMN and O_2 cofactors as in the previously described QM/MM MD simulations using TeraChem/NAMD. The MM part was treated with the CHARMM36 force field, but no cut-off or periodical boundary conditions were imposed unlike the case of MD calculations. The protein solvation box was trimmed to a water monolayer; therefore, the system contained 11445 atoms in total. No protein residues, ligands or water molecules were frozen during energy minimization. The typical step of the QM energy and gradient evaluation in the field of MM charges took ≈1.5–2 minutes to calculate with 16 OpenMP threads using TURBOMOLE, while DL-FIND optimizer iteration (including the MM energy and gradient evaluation) takes 0.3 seconds with 16 MPI processes. Thus, a typical calculation takes around

6 hours of wall time to reach convergence. Using all 16 cores allows for significant speedup of 10 times compared to a single core for both the TURBOMOLE and DL-FIND. If the starting conformation for the minimum energy search is taken from a MD frame with the oxygen molecule in pocket-1 (see Fig. 2), then the QM/MM minimum corresponds to the structure shown in the left side in Fig. 3 with the following distances: 3.05 Å for ND(Asn134)-O_2, 1.20 Å for O1-O2, 3.09 Å for O1-N5(FMN). The latter value is the most important result of this set of calculations. Consistently with the results of QM/MM MD simulations described above, this shows that the distance between any of the oxygen atom from O_2 to the N5 of FMN cannot be as low as 2.09 Å as reported in the crystal structure. The second approach to characterize the RutA-O_2 minimum energy structure using the QM/MM method was to apply the NWChem software package [4] implemented at the Lomonosov-2 supercomputer [27]. That NWChem 6.6 local installation was compiled with the ifort and icc (Intel Parallel Studio 2019) while using the MKL2019 and openmpi-4.0.1 libraries. Calculations were carried out utilizing 6–12 nodes per task (84 to 168 MPI processes). Few novel options were introduced as compared to the QM/MM calculations with TURBOMOLE/ChemShell. We considerably enlarged the QM-subsystem by including the almost entire FMN molecule, the oxygen molecule, fragments of the side chains of Lys 69, Trp139, Glu143, Glu292 and 15 water molecules (see the main frame in Fig. 4). We took the initial conformation for the structure optimization from the MD frame corresponding to the location of oxygen in pocket-5 of the complex (see Fig. 2). Now the selected groups in QM completely cover the interacting groups if the oxygen molecule is placed at the center of the QM-part. All other atoms of the model system are assigned to the MM part.
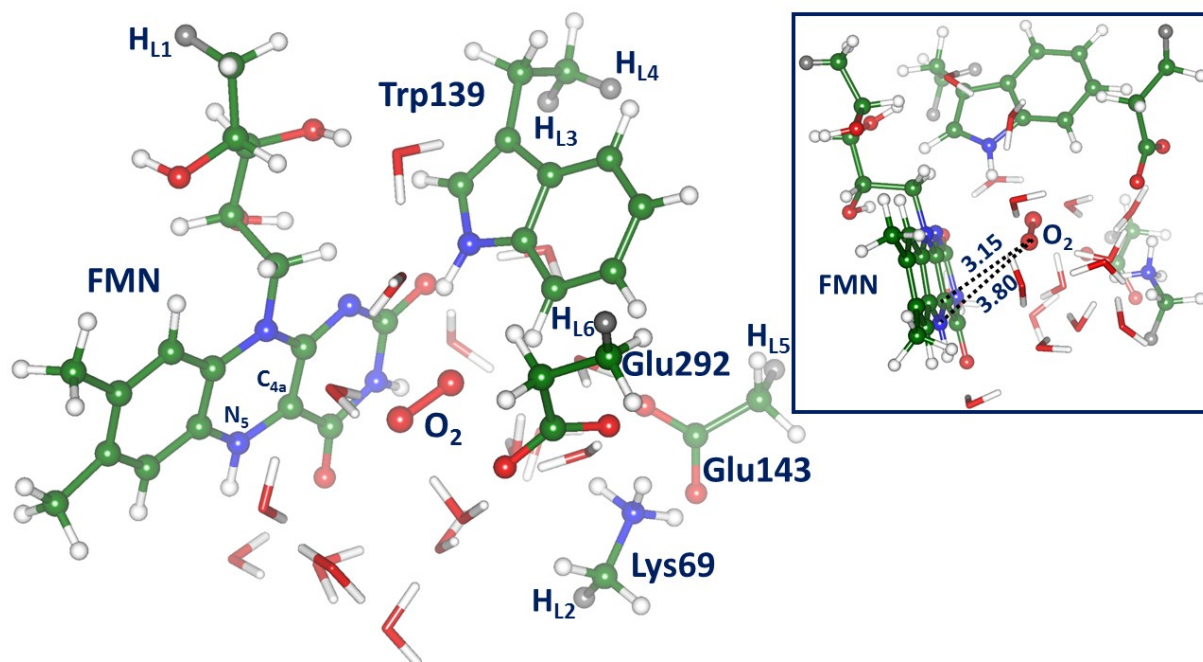

Figure 4. Molecular groups assigned to the quantum subsystem. The grey balls refer to the hydrogen link atoms ($HL_\#$) introduced to saturate the broken bonds C-O (HL_1), C-C (HL_2, HL_5, HL_6, HL_4) and C-N (HL_3) upon QM-MM partitioning. The inset in the right side shows the same subsystem in another perspective to emphasize that the oxygen molecule is located above the plane of the isoalloxazine ring of FMN. The distances from the oxygen atom of O_2 to the C4a and N5 atoms of FMN are given in Å

Finally, we used other approximations in the QM/MM scheme. On the base of the previous experience in modeling properties of flavin-containing photoactive proteins [20] we use here the density functional theory (DFT) approach with the PBE0 functional [2], the 6-31G* basis set, and the D3 dispersion correction [12] to compute energies and energy gradients in QM upon optimization geometry parameters of the model system. As before, to model the system in the triplet electronic state, the unrestricted DFT approach was used. The AMBER99 force field parameters [28] are employed to estimate energy and energy gradients in MM.

As shown in the very recent study [11], the treatment of the QM-MM boundary as well as of the embedding scheme is still an open question despite years of successful application of QM/MM codes in modern software packages. It seems that the only way to report results of QM/MM application that can be reproduced in subsequent simulations is to provide as many technical details as possible. Therefore, we explicitly point out that the hydrogen link atom scheme is applied here to saturate the dangling chemical bonds. These atoms and their positions are shown using the dark grey color in Fig. 4. Distances between the hydrogen link atoms and the partner atoms assigned to the QM part (here, all of them are the carbon atoms) are the same as in the $-CH_3$ groups.

The electrostatic embedding scheme is responsible for the interaction of the electron density in QM and the partial charges on MM atoms. To provide the necessary details, we note that NWChem performs a multi-region optimization procedure, i.e. at each optimization cycle, the QM region is optimized for M1 steps (10 in our calculations), whereas the MM region is optimized for M2 steps (300 in our case). If one applies the "density espfit" option in NWChem, this means that the electron density of the QM region is approximated with the electric charges obtained in the end of the QM part of the optimization cycle and used throughout the MM part. The "density static" option corresponds to the numerical integration to obtain the electron density of the QM region in the end of the QM part of each optimization cycle to use it during the MM part of that optimization cycle. Finally, we note that each link atom contacts the partner MM atom from the broken chemical bond. We employed in our calculations the NWChem option "mm charges exclude linkbond", which means that all the MM point charges are taken into consideration except the very ones located on the covalent QM/MM boundary. These MM point charges are set to zero. As mentioned above, these computational details are necessary to make the results reproducible.

The inset in Fig. 4 shows that the located equilibrium geometry configuration corresponds to the location of the oxygen molecule near the isoalloxazine ring of FMN. The computed distance between the closest to the ring oxygen atom and the C4a atom of flavin is 3.15 Å, whereas the O-N5 distance is 3.80 Å. The corresponding distances in the crystal structure PDB ID 6SGG are 3.11 Å and 2.09 Å.

To sum up, we conclude that a variety of computational approaches applied in this work show that the complex of the flavin-dependent protein RutA is able to bind the oxygen molecule in protein cavities, thus by forming the active site suitable for oxidation reactions. One of the found oxygen-binding pockets is very close to the site identified by the O_2 pressurized crystallography experiments [18]. However, our calculations could not reproduce a rather short O(oxygen)-N5(FMN) distance 2.09 Å in the structure of RutA-O_2 complex reported by the results of crystallography experiments. The experimentally obtained value for the distance seems to be too short for a hydrogen bond, if N5 is protonated in the reduced from of FMN, and too long for a covalent bond, if one assumes a covalent binding of oxygen to the deprotonated nitrogen in FMN.

As location of a small molecule O_2 in protein cavities remains a challenging experimental task, we suggest that in order to obtain reliable results, experimental data should be combined with the results of appropriate computational approaches, including the results of computationally demanding quantum-based methods. This issue becomes even more critical, if the precise location of the oxygen molecule in the structure of the active site is considered as a crucial point defining possible reaction mechanisms of a flavin-containing monooxygenase [1, 17, 26].

Conclusion

We demonstrate the application of high-performance computational methods to model the puzzling biochemical reactions of molecular oxygen with proteins, taking the interaction of oxygen with the flavin-containing monooxygenase RutA as a representative example. The presence of the oxygen molecule in model systems considerably complicates studies of structure and dynamics of large protein macromolecules, especially taking into account that localization of oxygen in protein sites is a nontrivial experimental task. Application of a wide spectrum of computational approaches including classical and QM/MM-based molecular dynamics as well as QM/MM optimization allowed us to characterize the RutA-O_2 complex and to dispute the recently reported crystallography structure of this complex. We show how the computational strategies can be optimized to apply several modern software packages in molecular modeling (NAMD, NWChem, TeraChem, ChemShell) using their options, which are often hidden for a user.

Acknowledgements

References

1. Adak, S., Begley, T.P.: RutA-Catalyzed Oxidative Cleavage of the Uracil Amide Involves Formation of a Flavin-N5-oxide. Biochemistry 56(29), 3708–3709 (2017). https://doi.org/10.1021/acs.biochem.7b00493

2. Adamo, C., Barone, V.: Toward reliable density functional methods without adjustable parameters: The PBE0 model. The Journal of Chemical Physics 110(13), 6158–6170 (1999). https://doi.org/10.1063/1.478522

3. Aleksandrov, A.: A molecular mechanics model for flavins. Journal of Computational Chemistry 40(32), 2834–2842 (2019). https://doi.org/10.1002/jcc.26061

4. Aprà, E., Bylaska, E.J., de Jong, W.A., *et al.*: NWChem: Past, present, and future. The Journal of Chemical Physics 152(18), 184102 (2020). https://doi.org/10.1063/5.0004997

5. Auhim, H.S., Grigorenko, B.L., Harris, T.K., *et al.*: Stalling chromophore synthesis of the fluorescent protein venus reveals the molecular basis of the final oxidation step. Chem. Sci. 12, 7735–7745 (2021). `https://doi.org/10.1039/D0SC06693A`

6. Balasubramani, S.G., Chen, G.P., Coriani, S., *et al.*: Turbomole: Modular program suite for ab initio quantum-chemical and condensed-matter simulations. The Journal of Chemical Physics 152(18), 184107 (2020). `https://doi.org/10.1063/5.0004635`

7. Berman, H.M., Westbrook, J., Feng, Z., *et al.*: The Protein Data Bank. Nucleic Acids Research 28(1), 235–242 (2000). `https://doi.org/10.1093/nar/28.1.235`

8. Best, R.B., Zhu, X., Shim, J., *et al.*: Optimization of the additive charmm all-atom protein force field targeting improved sampling of the backbone ϕ, ψ and side-chain $\xi1$ and $\xi2$ dihedral angles. Journal of Chemical Theory and Computation 8(9), 3257–3273 (2012). `https://doi.org/10.1021/ct300400x`

9. Chai, J.D., Head-Gordon, M.: Long-range corrected hybrid density functionals with damped atomatom dispersion corrections. Phys. Chem. Chem. Phys. 10, 6615–6620 (2008). `https://doi.org/10.1039/B810189B`

10. Colloc′h, N., Gabison, L., Monard, G., *et al.*: Oxygen Pressurized X-Ray Crystallography: Probing the Dioxygen Binding Site in Cofactorless Urate Oxidase and Implications for Its Catalytic Mechanism. Biophysical Journal 95(5), 2415–2422 (2008). `https://doi.org/10.1529/biophysj.107.122184`

11. Giudetti, G., Polyakov, I., Grigorenko, B.L., *et al.*: How Reproducible are QM/MM Simulations? Lessons from Computational Studies of the Covalent Inhibition of the SARS-CoV-2 Main Protease by Carmofur. ChemRxiv (2022). `https://doi.org/10.26434/chemrxiv-2022-4mmdc`

12. Grimme, S., Antony, J., Ehrlich, S., Krieg, H.: A consistent and accurate ab initio parametrization of density functional dispersion correction (DFT-D) for the 94 elements H-Pu. The Journal of Chemical Physics 132(15), 154104 (2010). `https://doi.org/10.1063/1.3382344`

13. Humphrey, W., Dalke, A., Schulten, K.: VMD: Visual molecular dynamics. Journal of Molecular Graphics 14(1), 33–38 (1996). `https://doi.org/10.1016/0263-7855(96)00018-5`

14. Khrenova, M.G., Polyakov, I.V., Nemukhin, A.V.: Molecular dynamics of enzyme-substrate complexes in guanosine-binding proteins. Khimicheskaya Fizika 41(6), 66–72 (2022). `https://doi.org/10.31857/S0207401X22060061`

15. Kstner, J., Carr, J.M., Keal, T.W., *et al.*: DL-FIND: An Open-Source Geometry Optimizer for Atomistic Simulations. The Journal of Physical Chemistry A 113(43), 11856–11865 (2009). `https://doi.org/10.1021/jp9028968`

16. Loh, K.D., Gyaneshwar, P., Papadimitriou, E.M., *et al.*: A previously undescribed pathway for pyrimidine catabolism. Proceedings of the National Academy of Sciences 103(13), 5114–5119 (2006). `https://doi.org/10.1073/pnas.0600521103`

17. Massey, V.: Activation of molecular oxygen by flavins and flavoproteins. Journal of Biological Chemistry 269(36), 22459–22462 (1994). `https://doi.org/10.1016/S0021-9258(17)31664-2`

18. Matthews, A., Saleem-Batcha, R., Sanders, J.N., *et. al*: Aminoperoxide adducts expand the catalytic repertoire of flavin monooxygenases. Nature Chemical Biology 16(5), 556–563 (2020). https://doi.org/10.1038/s41589-020-0476-2

19. Melo, M.C.R., Bernardi, R.C., Rudack, T., *et al.*: NAMD goes quantum: an integrative suite for hybrid simulations. Nature Methods 15(5), 351–354 (2018). https://doi.org/10.1038/nmeth.4638

20. Nemukhin, A.V., Grigorenko, B.L., Khrenova, M.G., Krylov, A.I.: Computational challenges in modeling of representative bioimaging proteins: GFP-like proteins, flavoproteins, and phytochromes. The Journal of Physical Chemistry B 123(29), 6133–6149 (2019). https://doi.org/10.1021/acs.jpcb.9b00591

21. Nemukhin, A.V., Grigorenko, B.L., Polyakov, I.V., Lushchekina, S.V.: Computational modeling of the SARS-CoV-2 main protease inhibition by the covalent binding of prospective drug molecules. Supercomputing Frontiers and Innovations 7(3), 25–32 (2020). https://doi.org/10.14529/jsfi200303

22. Phillips, J.C., Hardy, D.J., Maia, J.D.C., *et al.*: Scalable molecular dynamics on CPU and GPU architectures with NAMD. The Journal of Chemical Physics 153(4), 044130 (2020). https://doi.org/10.1063/5.0014475

23. Seritan, S., Bannwarth, C., Fales, B.S., *et al.*: Terachem: A graphical processing unit-accelerated electronic structure package for large-scale ab initio molecular dynamics. WIREs Computational Molecular Science 11(2), e1494 (2021). https://doi.org/10.1002/wcms.1494

24. Shabalin, I.G., Porebski, P.J., Minor, W.: Refining the macromolecular model – achieving the best agreement with the data from X-ray diffraction experiment. Crystallography Reviews 24(4), 236–262 (2018). https://doi.org/10.1080/0889311X.2018.1521805

25. Sherwood, P., de Vries, A.H., Guest, M.F., *et al.*: QUASI: A general purpose implementation of the QM/MM approach and its application to problems in catalysis. Journal of Molecular Structure: THEOCHEM 632(1), 1–28 (2003). https://doi.org/10.1016/S0166-1280(03)00285-9

26. Teufel, R.: Flavin-catalyzed redox tailoring reactions in natural product biosynthesis. Archives of Biochemistry and Biophysics 632, 20–27 (2017). https://doi.org/10.1016/j.abb.2017.06.008

27. Voevodin, V.V., Antonov, A.S., Nikitenko, D.A., *et al.*: Supercomputer Lomonosov-2: Large scale, deep monitoring and fine analytics for the user community. Supercomputing Frontiers and Innovations 6(2), 4–11 (2019). https://doi.org/10.14529/jsfi190201

28. Wang, J., Cieplak, P., Kollman, P.A.: How well does a restrained electrostatic potential (RESP) model perform in calculating conformational energies of organic and biological molecules? Journal of Computational Chemistry 21(12), 1049–1074 (2000). https://doi.org/10.1002/1096-987X(200009)21:12<1049::AID-JCC3>3.0.CO;2-F

29. Wang, S., Hou, K., Heinz, H.: Accurate and compatible force fields for molecular oxygen, nitrogen, and hydrogen to simulate gases, electrolytes, and heterogeneous interfaces. Journal of Chemical Theory and Computation 17(8), 5198–5213 (2021). https://doi.org/10.1021/acs.jctc.0c01132